Design of a Dual-Band WiFi Antenna Using the Theory of Characteristic Modes and Nested Chinese Characters

Zhonggen Wang , Mingqing Wang * , Wenyan Nie

Posted Date: 31 July 2023

doi: 10.20944/preprints202307.2116.v1

Keywords: characteristic mode; Chinese characters; WiFi; high isolation

Article

Design of a Dual-Band WiFi Antenna Using the Theory of Characteristic Modes and Nested Chinese Characters

Zhonggen Wang [1], Mingqing Wang [1,*] and Wenyan Nie [2]

[1] School of Electrical and Information Engineering, Anhui University of Science and Technology, Huainan 232001, China; zgwang@ahu.edu.cn

[2] School of Mechanical and Electrical Engineering, Huainan Normal University, Huainan 232001, China; wynie5240@163.com

* Correspondence: mqwang@aust.edu.cn

Abstract: In this paper, a dual-band WiFi antenna and its Multiple Input Multiple Output (MIMO) system application is designed, fabricated, and measured based on the Chinese characters "Men" and "Wei". The antenna uses a 40×40×1.6 mm^3 Fr4 substrate to analyze the combinatorial structure of Chinese characters using the theory of characteristic modes (TCM), to optimize the antenna dimensions by analyzing the mode current distribution, and to broaden the antenna bandwidth by etching rectangular slots on the ground. The measured and simulated results show that the four-element MIMO antenna covers 5.68-8.01 GHz, the isolation between the antennas is higher than 20 dB in the working band, the Envelope Correlation Coefficient (ECC) and the channel capacity losses (CCLs)of the simulation is lower than 0.001 and 0.18 bits/s/HZ, respectively. The efficiency of the antenna is higher than 90%, and it can be used for WiFi communication band (5.8 GHz and 6 GHz).

Keywords: characteristic mode; Chinese characters; WiFi; high isolation

1. Introduction

With the rapid development of wireless communication systems and the increasing demand for low-latency, low-loss, and high-speed wireless devices, the deployment of WiFi (6 GHz) has gained significant attention from researchers worldwide due to its notable advantages such as wider channel bandwidth, low latency, and high-speed capabilities. Recently, MIMO antenna technology has emerged as a popular approach for enhancing wireless communication by enabling faster data transmission rates, improved reliability, and enhanced spectrum utilization efficiency, particularly in complex environments. Furthermore, MIMO technology helps to overcome the multipath fading effect in rich scattering environments. However, improving the isolation and reducing the radiation correlation of MIMO antennas is a challenging task. It is common to use parasitic elements [1,2] and DGS techniques [3,4] to improve isolation. Reference [5] proposed a dual-unit MIMO antenna that uses both parasitic element and DSG technology to achieve isolation of 15 dB. Reference [6] proposed a four-port square patch antenna. In order to reduce the size and improve the isolation between antennas, the decoupling technology of mixed metal wall and half-wavelength diagonal slot was adopted in this design, so that the isolation reached 15db. Reference [7] proposed a frequency-selective element structure placed between two radiating elements to reduce coupling and achieve isolation of 17 dB. Reference [8] proposed a grounding part at the bottom of the substrate to enhance the isolation performance of the designed MIMO antenna, and successfully improved the isolation degree to 19.5 dB. However, in traditional methods, antenna design often depends on the experience and intuition of researchers, which will be difficult to explain the working principle of the antenna and will take longer time.

TCM was proposed and developed by Garbacz and Harrington [9,10] in 1968. TCM is widely used to design Ultra-Wideband (UWB) antennas [11,12], 5G mobile phone antenna [13,14], Ultra

Preprints (www.preprints.org) | NOT PEER-REVIEWED | Posted: 31 July 2023 doi:10.20944/preprints202307.2116.v1

High-Frequency Radio Frequency Identification (UHF RFID) [15,16], and array antennas [17,18], many antennas also use characteristic modes to analyze WiFi band [19–22] antennas. TCM is preferred by many researchers for its unique analysis method, i.e., the mode significances (MS) and mode currents are analyzed to select the appropriate excitation method and the mode to be excited; moreover, the structure is optimized to make it meet the design requirements. Recently, some interesting patch antenna designs, using artistic Chinese characters, have been proposed, such as the Si character patch [23], the design of the Si as a radiation patch, while the larger metal ground plane with a certain distance from the substrate used to improve the antenna gain; the Meng character patch [24], the antenna is designed with a double L-shaped feed probe and some diode switching circuits. By switching the on-off of the diode, it can cover different channels and generate circular polarization in different directions; and the arranged combination of the Zhong-Guo patch [25], the patches are connected together by a feed network to form a two-element antenna array. In this paper, a single antenna model with a combination of internal and external Chinese characters is designed using TCM. Compared with the existing antenna structures in the above references, it has the characteristics of simple structure, and the four-element MIMO antenna isolation is greater than 20 dB, and in the WiFi band (5.8 GHz, 6 GHz), the antenna gain can reach 6.5dbi and the efficiency can reach 93%.

To sum up, this paper will be divided as follows: in Section 2, the overall structure of the four-element MIMO antenna is first introduced, followed by the design and analysis of the single antenna using the characteristic mode. Moreover, this section describes the design and analysis process of the MIMO antenna. Section 3 presents some parametric analysis, section 4 gives the measured antenna system performance, such as the S-parameters and the radiation patterns values. Finally, some conclusions and future work ideas are given in Section 5.

2. Design and Analysis of the Antenna

Figure 1 illustrates the final antenna consisting of a central isolation branch placed on the upper surface of the substrate, and four identical "Men (门)" and "Wei (卫)" structures rotating around the center point. The rectangular ground on the lower surface of the Fr4 substrate (ε_r = 4.4, tan δ= 0.02) represents a cross of the Chinese character "Wei" whereas the rest is located on the upper surface of the substrate; moreover, the Chinese character "Men" is located on the upper surface of the substrate and encloses "Wei". Firstly, the distribution of the resonant mode currents is derived by performing the characteristic mode analysis of the combined structure of the individual Chinese characters using Computer Simulation Technology (CST) software. The mode currents are then analyzed to determine the feeding method and they are slotted in the ground to extend the bandwidth of the antenna; therefore, the performance and frequency response of the antenna would improve. Then, the High-Frequency Structure Simulator (HFSS) software is used to construct a four-element MIMO antenna by a rotational replication operation for a single antenna. Finally, isolation branches are added to enhance the antenna isolation. The sizes of the antenna are provided in Table 1.

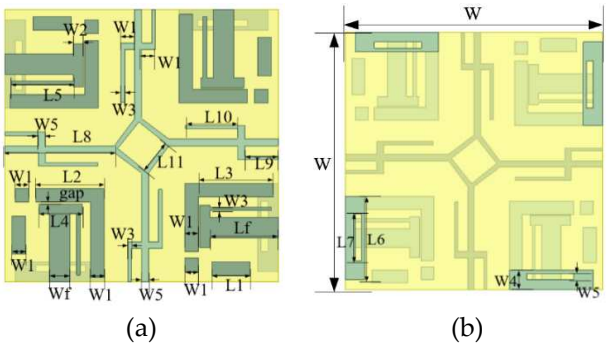

(a) (b)

Figure 1. Geometry and parameters of the proposed MIMO antenna: (a) front view, (b) back view.

Preprints (www.preprints.org) | NOT PEER-REVIEWED | Posted: 31 July 2023 doi:10.20944/preprints202307.2116.v1

Table 1. Recommend design dimensions for antenna.

Parameter	W	W1	W2	W3	W4	W5	Wf	Lf	Gap	L1
Value/mm	20	2	1.5	0.5	3	1	3	10	0.2	5.6
Parameter	L2	L3	L4	L5	L6	L7	L8	L9	L10	L11
Value/mm	10	11	6.3	9	13	7.3	16	4.9	7.7	5

2.1. Design and analysis of a single antenna base on the TCM

Figure 2 shows the evolution of the antenna structure of one unit where the antenna uses an Fr4 substrate of size 40×40×1.6 mm^3. The modeling and characteristic mode analysis of the initial structure of the antenna, using the commercial CST soft-ware, is represented in Figure 2(a).

In the characteristic mode theory, MS and CA is an important parameter, it can be calculated using this equation:

$$\mathrm{MS} = \left|1/(1+\mathrm{j}\lambda_n)\right| \tag{1}$$

$$CA = \pi - \tan^{-1}(\lambda_n) \tag{2}$$

When the MS value is greater than 0.707, the antenna is operating in a potentially excitable resonant mode [26]; however, when MS is close to zero, the mode is difficult to excite. When considering MS, CA also needs to be considered, and when CA is close to 180°, it indicates that the mode is prone to resonance [27]. The MS and characteristic angle (CA) comparison plots before and after the evolution of the first three modes are given in Figure 3. According to the MS and CA curves of model I in Figure 3, the resonance frequencies of the initial structure are 4.035 GHz, 5.965 GHz and 7.015 GHz, respectively.

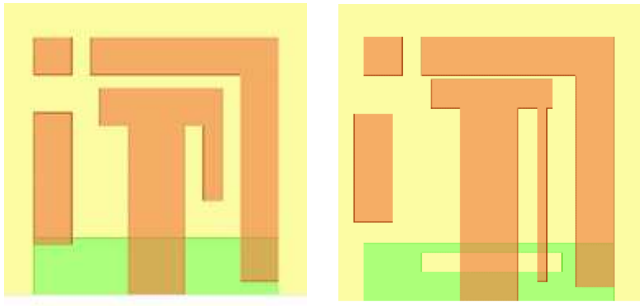

(a) (b)

Figure 2. The evolution of the antenna: (a) model I-Original structure, (b) model II-Final single antenna structure.

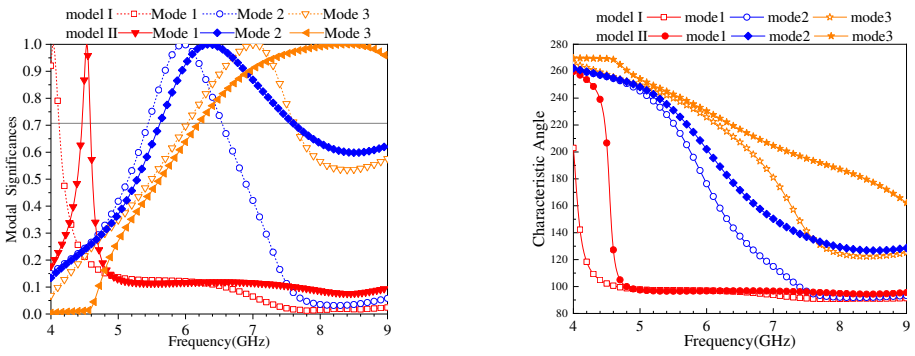

(a) (b)

Figure 3. MS and CA for the first three modes: (a)MS, (b)CA.

Preprints (www.preprints.org) | NOT PEER-REVIEWED | Posted: 31 July 2023 doi:10.20944/preprints202307.2116.v1

As for Figure 4, it shows the current distribution in the resonant mode. The cur-rent of Mode 1 is mainly located on the feeder, the ground, and the right branch of the "Men" whereas the Mode 2 current is mainly concentrated in the feeder and the Mode 3 currents are mainly located on the ground and in the upper right corner of the radiator. Feeding two separate modes to increase the bandwidth is not always possible due to the ideal feed types, locations, and impedances that can be very different from each other [28], thus, it can be derived from the resonant mode currents that Mode 1 and Mode 2 are more likely to be fed using the same excitation.

The primary focus of this paper revolves around the WiFi band, mainly centered on optimizing Mode 2. By analyzing the current distribution of Mode 2, it was observed that the current on the ground plane exhibited relatively weaker intensity. To alter the current strength and optimize the microstrip antenna structure, a slotting technique was applied in this research. Specifically, rectangular slots were etched at the positions where the ground plane current was minimal. The current distribution of mode 2 after slotting is depicted in Figure 4(e). It is evident from Figure 4 that slotting enhances the current on the ground plane. Furthermore, with reference to Figure 3, the proposed mode 2 antenna exhibits a broader bandwidth compared to the initial structure.

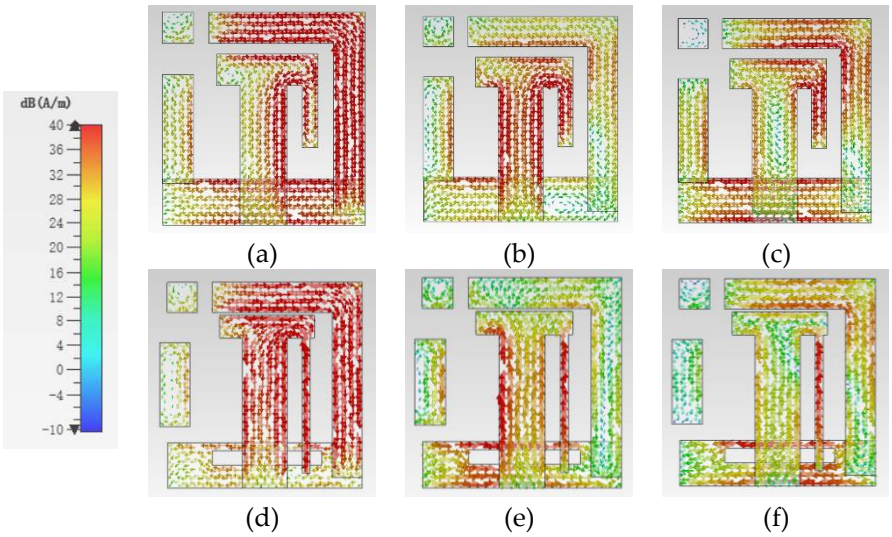

Figure 4. Model I and model II currents at resonant mode where, for model I: (a) Mode 1 at 4.035 GHz, (b) Mode 2 at 5.965 GHz, (c) Mode 3 at 7.015 GHz, and for model II: (d) Mode 1 at 4.535 GHz, (e) Mode 2 at 6.35 GHz, (e) Mode 3 at 8.385 GHz.

The antenna is feed by a 50 Ω microstrip feed line. The S-parameters and the gain of the single-port antenna simulation are shown in Figure 5, the antenna covers the frequency range of 5.67-7.99 GHz and can cover the WiFi range (5.8 GHz, 6 GHz); as for the gain of the working band, it is in the range 2.24-2.81 dBi. In addition, Figure 5 also shows a comparison of the S-parameters before and after the slotted ground where, after etching the rectangular slot, not only the bandwidth is increased, but also the matching performance is better.

Preprints (www.preprints.org) | NOT PEER-REVIEWED | Posted: 31 July 2023 doi:10.20944/preprints202307.2116.v1

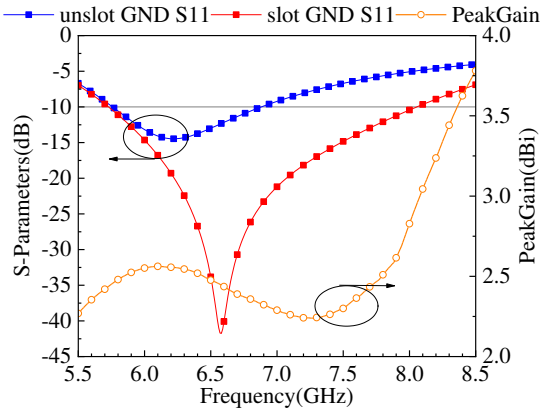

Figure 5. Simulated single antenna S-parameters and gain.

2.2. MIMO antenna design and analysis

Referring to Figure 6 (a), the designed single antenna rotates around the center point to form a four-element MIMO antenna called Model III. As for Figure 6 (b), to further reduce the coupling between antennas, an isolated branch is designed in this paper where the MIMO antenna is called Model IV. Moreover, the isolated branch is composed of a diamond ring, a rectangle leading from each diamond corner, and a z-shape attached to the rectangle. Finally, Figure 7 shows the fabricated prototype, and the relevant parameters of the branch are shown in Table 1.

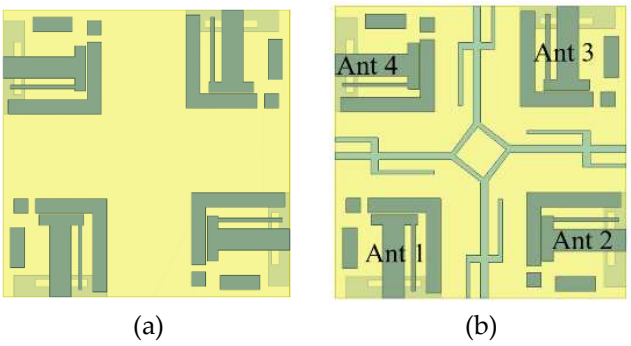

Figure 6. Design of MIMO antennas: (a)model III, (b) model IV.

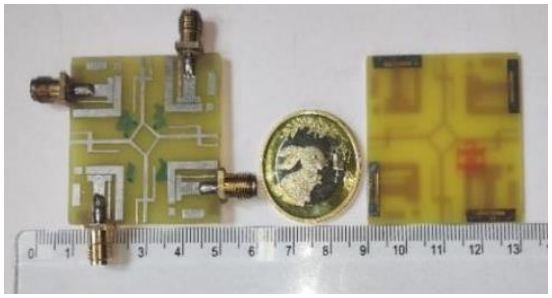

Figure 7. Fabrication prototype of the proposed four-port MIMO antenna.

Figure 8 shows the comparison of the S-parameters before and after adding the isolation branches. From S11, the antenna coverage frequency is expanded from 5.7-7.84 GHz to 5.61-8.18 GHz, but it was found that the frequency was shifted before the isolated branches were added. This was mainly due to the rotation and replication process of the antenna radiating body that will introduce certain interference and mismatch, resulting in the alteration of the antenna performance. Concerning S12 and S13, the isolation degree is improved in the covered band. Furthermore, the added isolation branches not only improve the isolation degree and reduce the crosstalk, but they also generate new

Preprints (www.preprints.org) | NOT PEER-REVIEWED | Posted: 31 July 2023 doi:10.20944/preprints202307.2116.v1

high-frequency resonance to expand the high-frequency band-width and improve the signal transmission performance and spectral utilization efficiency. The current distribution on the antenna surface is presented in Figure 9. At 6.06 GHz and 7.48 GHz frequencies, when port 1 is excited and the other ports are cut off with a matching load of 50 Ω, the isolation branch blocks the majority of the current, thus reducing the coupling and improving the isolation of the MIMO antenna.

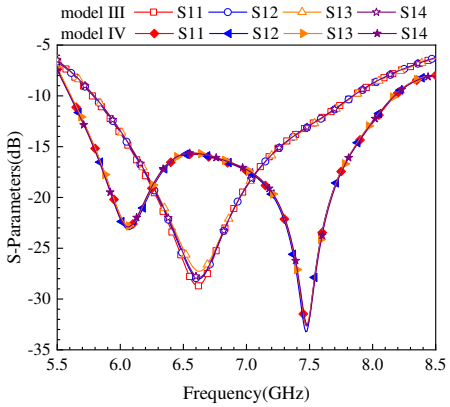

Figure 8. Effect of isolated branch on S-parameters.

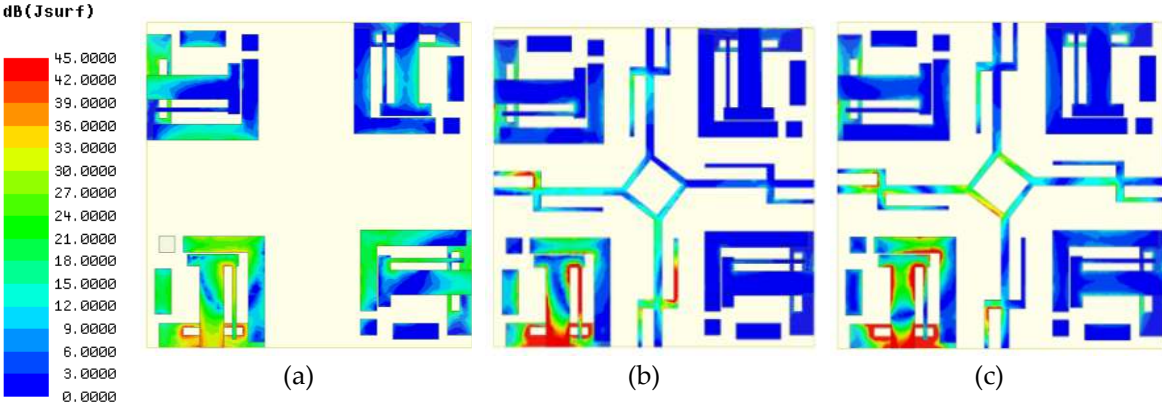

Figure 9. Surface current distribution of (a) model III at 6.6 GHz, (b) model IV at 6.06 GHz, (c) model IV at 7.48 GHz.

3. Parametric Study

To examine the effect of different parameters of antenna on its performance, a systematic study is carried out. The goal of this study is to identify the fabrication tolerance, and more importantly, to pinpoint the effects of antenna parameters on the bandwidth. We investigated the effects of ground slot length L7, gap width, and isolation branch length L8 on antenna performance. The first two parameters are selected because they establish the framework of a single antenna structure, while the last parameter plays an important role in improving the isolation of MIMO antenna systems.

As shown in Figure 10, the width of the gap affects the coupling degree between the WEI patch and the MEN patch. When gap=0.2 mm, the performance of the S parameter is the best. As the gap increases, there is a certain performance decrease in both bandwidth and matching degree of the antenna, which becomes more obvious with the increase of distance. Smaller gaps can enhance the coupling between them and thus improve the performance of the antenna. When the gap increases, the electromagnetic coupling is weakened, leading to a decrease in the bandwidth and matching of the antenna. As shown in Figure 11, the ground slotting has a certain influence on the bandwidth of the antenna, which shows that when L7 increases from 5.3 mm to 7.3 mm in length, the bandwidth of the antenna widens with the increase in length and the better match, but when it continues to increase to 8.3 mm, the bandwidth of the antenna decreases close to 1 GHz. this may be because when

Preprints (www.preprints.org) | NOT PEER-REVIEWED | Posted: 31 July 2023 doi:10.20944/preprints202307.2116.v1

the slotting length exceeds a certain threshold, the introduced structural changes cause the resonant frequency of the antenna to deviate from expected, resulting in the bandwidth of the antenna being limited and the signal not being transmitted to a higher frequency range.

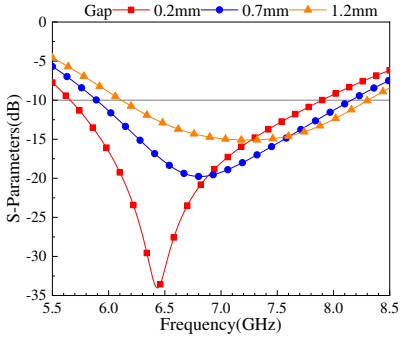

Figure 10. Effect of gap on S-parameters.

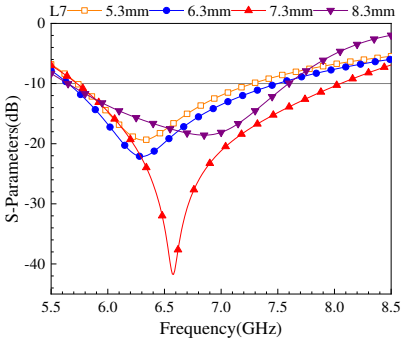

Figure 11. Effect of slotted length L7 on S-parameters.

The isolation branch of the MIMO antenna plays a crucial role in the isolation degree of the antenna, as in Figure 12, when the length of the branch L8 is 8 mm, the S11 parameter of the antenna is higher than -10 dB, which may be caused by the mismatch between the length of the isolation branch and the operating frequency range of the antenna element, thus causing an impedance mismatch and reducing the performance of the antenna. As the length increases, the S parameter of the antenna tends to be stable, and the isolation of the antenna further decreases to below -20 dB.

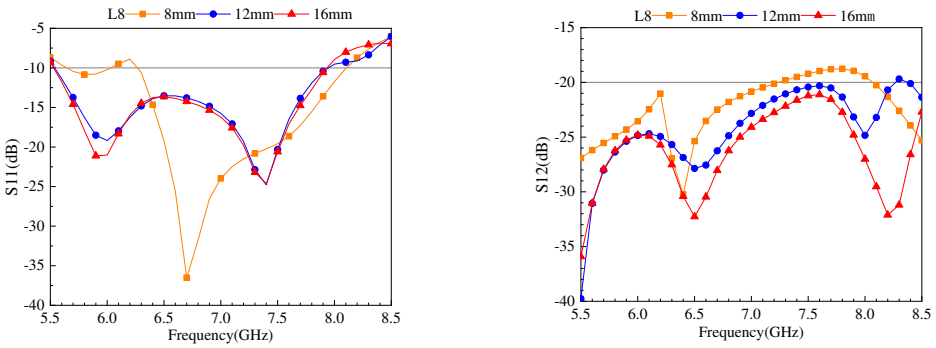

Figure 12. Effect of isolated branch length L8 on S parameters: (a)S11; (b)S12.

Preprints (www.preprints.org) | NOT PEER-REVIEWED | Posted: 31 July 2023 doi:10.20944/preprints202307.2116.v1

4. Measurement and Simulation Results

The S-parameters are measured using an AV3629D vector network analyzer and Figure 13 shows the far-field measured environment. Figure 14 shows the simulated and measured S-parameters results. These findings show that the antenna can cover the bandwidth range 5.68-8.01 GHz, with an isolation degree of 20 dB. However, there are differences between the simulated and the measured, which may be due to soldering errors and manufacturing tolerances.

Figure 13. The environment of the model measurement.

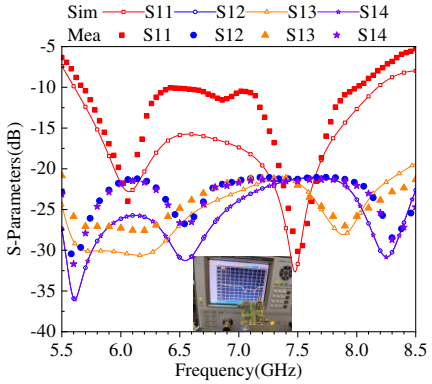

Figure 14. S-Parameters of proposed MIMO antenna.

Furthermore, the antenna was tested for its radiation patterns in an anechoic chamber. Since the four antenna elements are identical, only the radiation pattern of Ant-1 was measured, and the rest of the ports were replaced by a 50 Ω load matching. The radiation direction diagram of the antenna was tested in the anechoic chamber as presented in Figure 15, which shows the simulated and measured EH plane direction maps in the resonant mode at 6.06 GHz and 7.48 GHz. The simulated and measured results are matching. Moreover, Figure 16 shows the peak gain and the antenna efficiency for the pro-posed MIMO system where the antenna gains ranges between 2.5 and 6.5 dBi and the MIMO antenna efficiency varies between 79% and 93%. Furthermore, the gain in the WiFi band varies between 4.73 and 6.5 dBi and its efficiency is in the range of 90%-93%.

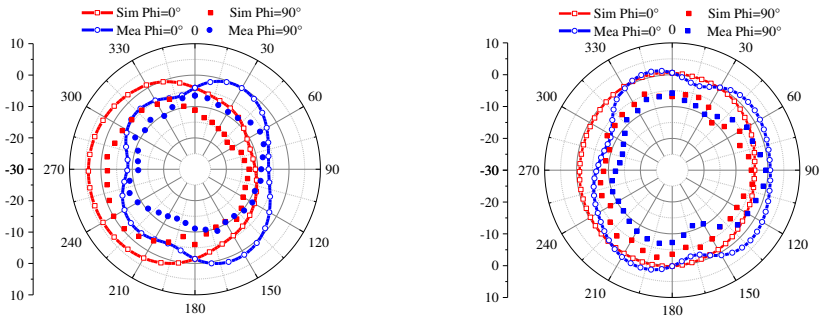

Preprints (www.preprints.org) | NOT PEER-REVIEWED | Posted: 31 July 2023 doi:10.20944/preprints202307.2116.v1

Figure 15. Simulated and measured radiation patterns results of the proposed single-port MIMO antenna under Ant-1 excitation: (a) at 6.06 GHz, (b) at 7.48 GHz.

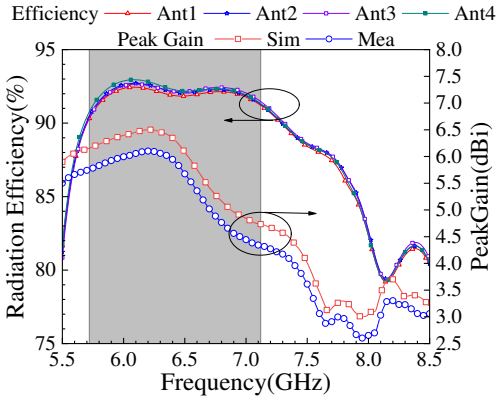

Figure 16. Efficiency and gain of the proposed MIMO antenna.

The degree of the channel isolation of a MIMO antenna can be measured by the ECC technique where a lower ECC indicates a higher pattern diversity of the antenna. The ECC data is calculated by using the S-parameters through (3) [29]. Diversity gain (DG) is an important measure of how much the signal is amplified or attenuated in a MIMO system. It can be expressed by the ECC as Equation (4). In generally, The ECC of the MIMO antenna is generally lower than 0.5, which is considered to comply with the requirements, and the closer the DG is to 10 the better the performance of the MIMO antenna. Figure 17 shows the simulated ECC and DG of the proposed MIMO system, and the results show that the proposed four-element MIMO antenna system has both a larger DG and a smaller ECC. The ECC of the studied and designed antenna in this paper is lower than 0.001 in the WiFi band.

$$ECC_{i,j} = \frac{\left|S_{ii}^{*}S_{ij} + S_{ji}^{*}S_{jj}\right|^{2}}{\left(1-\left|S_{ii}\right|^{2}-\left|S_{ji}\right|^{2}\right)\left(1-\left|S_{jj}\right|^{2}-\left|S_{ij}\right|^{2}\right)} \tag{3}$$

$$DG = 10\times\sqrt{1-ECC^{2}} \tag{4}$$

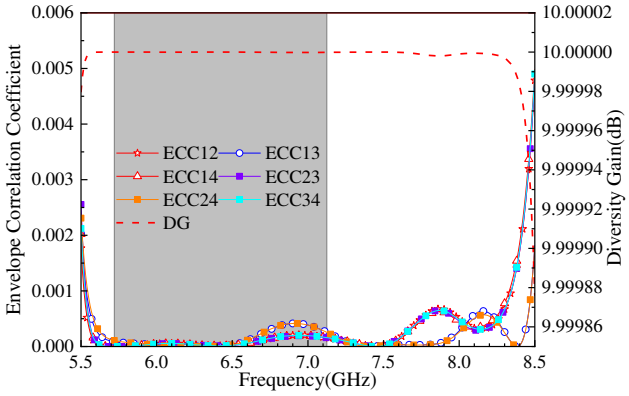

Figure 17. ECC and DG of the proposed MIMO antenna.

In addition, the total active reflection coefficient (TARC) and CCLs are investigated in this paper. The TARC value falls within the range of 0 to 1, wherein a value nearing 0 signifies minimal reflection power and a value nearing 1 signifies significant reflection power. The proximity of the TARC value to 0 indicates superior system performance, as it implies the efficient transmission of energy to the

Preprints (www.preprints.org) | NOT PEER-REVIEWED | Posted: 31 July 2023 doi:10.20944/preprints202307.2116.v1

receiving end, minimizing reflection or loss. These parameters are computed using Equations (5) to (7) given below [30–32]., and Figure 18 shows the TARC and the CCL calculations for the pro-posed MIMO antenna, which shows that the TARC is below 30 dB, and the CCL is be-low 0.18 bits/s/HZ in the operating band. This fully reflects the high performance characteristics of MIMO antenna system.

$$TARC = -\sqrt{\frac{\left|(S_{11}+S_{12}e^{j\theta})^2\right|+\left|(S_{21}+S_{22}e^{j\theta})^2\right|}{2}} \tag{5}$$

$$CCL = -\log_2 \det(\alpha^R)$$
$$\alpha^R = \begin{bmatrix} \alpha_{11} & \alpha_{12} \\ \alpha_{21} & \alpha_{22} \end{bmatrix} \tag{6}$$

where,

$$\alpha_{11}=1-(|S_{11}|^2+|S_{12}|^2); \quad \alpha_{12}=-S_{11}*S_{12}-S_{21}*S_{22}$$
$$\alpha_{22}=1-(|S_{22}|^2+|S_{21}|^2); \quad \alpha_{21}=-S_{22}*S_{21}-S_{12}*S_{11} \tag{7}$$

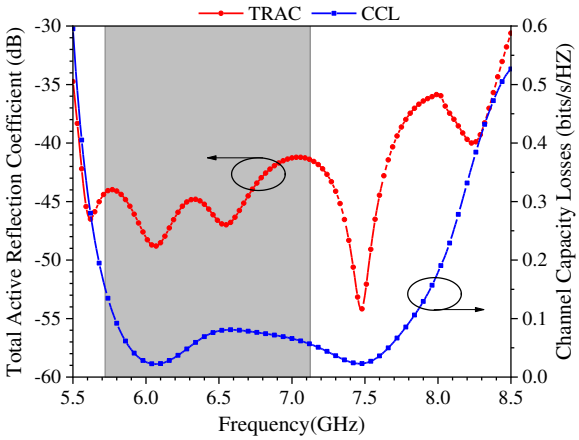

Figure 18. Proposed 4-element the TARC and the CCL diversity performance.

Finally, Table 2 shows the dimensions, the operating band, peak gain, the mini-mum isolation, the efficiency, the ECC, the TARC, and the CCL of the proposed antenna which are compared with some previously reported MIMO antennas. The antenna structure proposed in this paper has a small antenna size, and the isolation of the proposed MIMO antenna system reaches 20 dB in the frequency band, and the efficiency can reach 93% with an ECC below 0.001. It is clear that the proposed design is very compact and performs well.

Table 2. Antenna Parameter Comparison.

Ref	Size (mm^3)	Band (GHz)	Peak Gain (dB)	Min-Isolation (dB)	Min-Efficiency (%)	ECC	TARC (dB)	CCL
[1]	11×14×1.6	5.2-5.33	5.83	18	/	<0.004	<14.5	0.35
[2]	25×25×1.57	3.4–3.6 5.15–5.85	/	>19.8	/	<0.06	/	/
[5]	50×40×1.59	2.12–2.8 4.95-6.65	6.4	>15	/	<0.01	/	/

[6]	50×50×11.2	2.4-2.5 5.15-7.125	4.0-5.9	>20	>86	<0.01	/	/
[8]	50×50×1.6	2.25–2.9 5.05–6.025	3.8	>19.3	>61.4	<0.03	/	/
[19]	$\pi\times18^2\times7$	2.4-2.49	3.5	>20	>75	<0.014	/	/
[21]	55×55×1.56	5.7-5.9	5.3	>32	>84	<0.0001	<-10	<0.1
[22]	120×50×5.4	2.25-2.63 5.14-6.06	5.2 6.7	>17.5	>81	<0.12	/	/
[30]	72×72×1.6	5.14-6.06	>2.5	>15	>95	<0.005	<-10	<0.05
[31]	44×31×1.6	2.28–2.47 3.34–3.73 4.57–6.75	1.3 2.9 4.3	>20	/	<0.002	/	/
[32]	22.5×50×3.5	5.2-6.4	6	>18	72-84	<0.001	/	/
This work	40×40×1.6	5.68-8.01	2.5-6.5	>20	79-93	<0.001	<-30	<0.18

5. Conclusions

In this paper, the design of the "Men Wei" antenna, based on the characteristic mode theory and its MIMO system application, is proposed. The antenna's size is 40×40×1.6 mm^3, and the commonly used Fr4 substrate is used, which is characterized by its easy processing and low cost. As for the simulated and measured results, they show that the antenna and MIMO system have versatility and better performance, such as miniaturization, high isolation, and low envelope correlation coefficient. Finally, the designed antenna can be applied to WiFi (5.8 GHz, 6 GHz) devices.

Author Contributions: Conceptualization, Z.W.; methodology, M.W.; Simulation, M.W.; validation, M.W. and W.N.; writing—review and editing, Z.W. and W.M.; data curation, W.N. All authors have read and agreed to the published version of the manuscript.

Funding: This research was funded by the Anhui Provincial Natural Science Foundation of China under Grant no. 2108085MF200, in part by the Natural Science Foundation of Anhui Provincial Education Department under Grant no. 2022AH051583, in part by the Anhui Province Graduate Academic Innovation Project under grant no. 2021200851.

Conflicts of Interest: The authors declare no conflict of interest.

References

1. Vinay S., Ananya G., Madhur D. U., et al. "A Pi-Shaped Slot Antenna for 5.2 GHz WLANMIMO Application", *IETE Journal of Research*, vol.69, no.3, pp. 1613-1625, 2023.
2. Paiva, S.B.; Junior, A.G.D.; Neto, V.P.S., et al. "A New Compact Dual-Polarized MIMO Antenna Using Slot and Parasitic Element Decoupling for 5G and WLAN Applications. " *Electronics*, vol. 11, no. 13: 1943, 2022.
3. M. F. Nakmouche, D. Deslandes and G. Gagnon, "Dual-Band 4-Port H-DGS Based Textile MIMO Antenna Design Using Genetics Algorithms for Wearable Application," *2022 IEEE International Symposium on Antennas and Propagation and USNC-URSI Radio Science Meeting (AP-S/URSI)*, Denver, CO, USA, 2022, pp. 1182-1183.
4. Malaisamy, K., Santhi, M., Robinson, S. "Design and analysis of 4 × 4 MIMO antenna with DGS for WLAN applications." *International Journal of Microwave and Wireless Technologies*, vol. 13, no. 9, pp. 979-985, 2021.
5. Peng H, Zhi R, Yang Q, et al. "Design of a MIMO Antenna with High Gain and Enhanced Isolation for WLAN Applications." *Electronics*, vol. 10, no. 14:1659, 2021.
6. Wong, K. L.; Jiang, H. Y.; Li, W. Y, "Decoupling Hybrid Metal Walls and Half-Wavelength Diagonal Open-Slots Based Four-Port Square Patch Antenna With High Port Isolation and Low Radiation Correlation for 2.4/5/6 GHz WiFi-6E 4 × 4 MIMO Access Points," *IEEE Access*, vol. 10, pp. 81296-81308, 2022.
7. Saha, P.B.; Ghoshal, D.; Dash, R.K., "Frequency Selective Meta-Structure Embedded Two-Element MIMO Antenna with Enhanced Isolation and Pattern Diversity for WLAN/WiMAX Applications." *ETE Journal of Research*, vol. 69, no. 5, pp. 2999-3010, 2021.
8. Yang Q, Zhang C, Cai Q, Loh TH, Liu G. A MIMO Antenna with High Gain and Enhanced Isolation for WLAN Applications. *Applied Sciences*. Vol. 12, no. 5:2279, 2022.
9. R. Garbacz and R. Turpin, "A generalized expansion for radiated and scattered fields," *IEEE Transactions on Antennas and Propagation*, vol. 19, no. 3, pp. 348-358, May 1971.

10. R. Harrington and J. Mautz, "Theory of characteristic modes for conducting bodies," *IEEE Transactions on Antennas and Propagation*, vol. 19, no. 5, pp. 622-628, September 1971.
11. Q. Zhang, R. Ma, W. Su and Y. Gao, "Design of a Multimode UWB Antenna Using Characteristic Mode Analysis," *IEEE Transactions on Antennas and Propagation*, vol. 66, no. 7, pp. 3712-3717, July 2018.
12. X. Zhao, S. P. Yeo and L. C. Ong, "Planar UWB MIMO Antenna With Pattern Diversity and Isolation Improvement for Mobile Platform Based on the Theory of Characteristic Modes," *IEEE Transactions on Antennas and Propagation*, vol. 66, no. 1, pp. 420-425, Jan. 2018.
13. H. H. Zhang et al., "Low-SAR MIMO Antenna Array Design Using Characteristic Modes for 5G Mobile Phones," *IEEE Transactions on Antennas and Propagation*, vol. 70, no. 4, pp. 3052-3057, April 2022.
14. H. H. Zhang, X. Z. Liu, G. S. Cheng, Y. Liu, G. M. Shi and K. Li, "Low-SAR Four-Antenna MIMO Array for 5G Mobile Phones Based on the Theory of Characteristic Modes of Composite PEC-Lossy Dielectric Structures," *IEEE Transactions on Antennas and Propagation*, vol. 70, no. 3, pp. 1623-1631, March 2022.
15. A. Sharif et al., "Low-Cost Inkjet-Printed UHF RFID Tag-Based System for Internet of Things Applications Using Characteristic Modes," *IEEE Internet of Things Journal*, vol. 6, no. 2, pp. 3962-3975, April 2019.
16. A. Sharif et al., "UHF RFID Tag Design Using Theory of Characteristics Modes for Platform-Tolerant and Harsh Metallic Environments," *IEEE Journal of Radio Frequency Identification*, vol. 6, pp. 524-533, August 2022.
17. K. R. Jha, N. Rana and S. K. Sharma, "Design of Compact Antenna Array for MIMO Implementation Using Characteristic Mode Analysis for 5G NR and Wi-Fi 6 Applications," *IEEE Open Journal of Antennas and Propagation*, vol. 4, pp. 262-277, February 2023.
18. W. Liu and S. Yan, "A Design of Millimeter-Wave Dual-Polarized SIW Phased Array Antenna Using Characteristic Mode Analysis," *IEEE Antennas and Wireless Propagation Letters*, vol. 21, no. 1, pp. 29-33, Jan. 2022.
19. D. Wen, Y. Hao, H. Wang and H. Zhou, "Design of a MIMO Antenna With High Isolation for Smartwatch Applications Using the Theory of Characteristic Modes," IEEE Transactions on Antennas and Propagation, vol. 67, no. 3, pp. 1437-1447, March 2019.
20. H. H. Zhang, et al., "Design of Low-SAR and High On-Body Efficiency Tri-Band Smartwatch Antenna Utilizing the Theory of Characteristic Modes of Composite PEC-Lossy Dielectric Structures," *IEEE Transactions on Antennas and Propagation*, vol. 71, no. 2, pp. 1913-1918, Feb. 2023.
21. E. Fritz-Andrade, A. Perez-Miguel, R. Gomez-Villanueva, et al. "Characteristic mode analysis applied to reduce the mutual coupling of a four-element patch MIMO antenna using a defected ground structure," *IET Microwaves Antennas Propagation*, vol. 14, no. 2, pp. 215-226, Feb. 2020.
22. W. Zhang, Y. Li, K. Wei and Z. Zhang, "A Dual-Band MIMO Antenna System for 2.4/5 GHz WLAN Applications," *IEEE Transactions on Antennas and Propagation*, vol. 71, no. 7, pp. 5749-5758, July 2023.
23. W. Zhou, C. Yue, Y. Li, Y. Xia, B. Qiu and K. L. Chung, "A High Gain Si-shaped Circularly Polarized Patch Antenna for 5G Application," *2021 IEEE 4th International Conference on Electronic Information and Communication Technology (ICEICT)*, Xi'an, China, 2021, pp. 284-285.
24. K. L. Chung, S. Xie, Y. Li, R. Liu, S. Ji and C. Zhang, "A Circular-Polarization Reconfigurable Meng-Shaped Patch Antenna," *IEEE Access*, vol. 6, pp. 51419-51428, 2018.
25. K. L. Chung, W. Li, Y. Li, R. Liu and P. Zhang, "Chinese Character-Shaped Artistic Patch Antenna," *IEEE Antennas and Wireless Propagation Letters*, vol. 18, no. 8, pp. 1542-1546, Aug. 2019.
26. C. Wang, Y. Chen and S. Yang, "Bandwidth Enhancement of a Dual-Polarized Slot Antenna Using Characteristic Modes," *IEEE Antennas and Wireless Propagation Letters*, vol. 17, no. 6, pp. 988-992, June 2018.
27. J. Zeng, X. Liang, L. He, F. Guan, F. H. Lin and J. Zi, "Single-Fed Triple-Mode Wideband Circularly Polarized Microstrip Antennas Using Characteristic Mode Analysis," *IEEE Transactions on Antennas and Propagation*, vol. 70, no. 2, pp. 846-855, Feb. 2022.
28. Z. Miers, H. Li and B. K. Lau, "Design of Bandwidth-Enhanced and Multiband MIMO Antennas Using Characteristic Modes," *IEEE Antennas and Wireless Propagation Letters*, vol. 12, pp. 1696-1699, November 2013.
29. Y. Y. Liu and Z. H. Tu, "Compact Differential Band-Notched Stepped-Slot UWB-MIMO Antenna With Common-Mode Suppression," *IEEE Antennas and Wireless Propagation Letters*, vol. 16, pp. 593-596, 2017.
30. Addepalli, T.; Kumar, M.S.; Jetti, C.R., et al. "Fractal Loaded, Novel, and Compact Two- and Eight-Element High Diversity MIMO Antenna for 5G Sub-6 GHz (N77/N78 and N79) and WLAN Applications, Verified with TCM Analysis," *Electronics*, vol. 12, no. 4: 952, 2023.
31. Bayarzaya, B.; Hussain, N.; Awan, W.A., et al. "A Compact MIMO Antenna with Improved Isolation for ISM, Sub-6 GHz, and WLAN Application, " *Micromachines*, vol. 13, no. 8: 1355, 2022.
32. Khan, I.; Wu, Q.; Ullah, I., et al. "Designed Circularly Polarized Two-Port Microstrip MIMO Antenna for WLAN Applications," *Sciences*, vol. 12, no. 3: 1068, 2022.